Available online at https://jamda.abru.ac.ir/
Journal of Applied Mathematics & Data Analytics
Vol. 2, No. 2, 2026, 48–59
Research Article

Ridge-Regularised Fourier Autoregression for Periodic Climate Time Series: Simulation Evidence and an Application to Nigerian Rainfall and Humidity

Felix Azuka Okolie*
Department of Mathematical Sciences, Ajayi Crowther University, Oyo, Nigeria

Abass Ishola Taiwo
Department of Statistics, Olabisi Onabanjo University, Ago-Iwoye, Nigeria

Timothy Olabisi Olatayo
Department of Statistics, Olabisi Onabanjo University, Ago-Iwoye, Nigeria

Abstract

Abstract: This study develops a ridge-regularised Fourier autoregressive (Ridge-PFAR) model for periodic climate series in which harmonic lag regressors can become numerous and strongly correlated. A 500-replication Monte Carlo experiment compares unpenalised Fourier autoregression (FAR) and Ridge-PFAR at a fixed sample size and forecast horizon under low-, moderate-, and high-dimensional designs. In the high-dimensional design, FAR produces severe forecast outliers, with a median 24-step RMSE of 10.9645 and a mean RMSE of 2621.5584, whereas Ridge-PFAR reduces these values to 1.1576 and 1.1874, respectively. The median normal-equation condition number decreases from 3049.0586 to 7.2537 after regularisation. The empirical analysis uses 132 monthly Nigerian observations from January 2014 to December 2024, with the first 108 observations used for model selection and the final 24 reserved for testing. All combinations $p = 1, \ldots, 10$ and $K = 1, \ldots, 4$ are assessed using identical rolling-origin folds, and a seasonal-naive forecast provides a practical benchmark. For rainfall, FAR yields the lowest test RMSE (53.8078), followed by Ridge-PFAR (56.6733) and the seasonal-naive method (60.7139). For relative humidity, Ridge-PFAR lowers the RMSE to 5.8410, compared with 6.2069 for FAR and 8.2031 for the seasonal-naive method. The 95% residual-bootstrap intervals achieve test-period coverage of 95.83% for rainfall and 87.50% for relative humidity. The results indicate that ridge regularisation is an effective safeguard against severe high-dimensional instability, although its forecasting gains in the empirical application remain target-dependent.

Keywords: climate forecasting, Fourier autoregression, multicollinearity, periodic time series, ridge regularisation, rolling-origin validation.
2020 Mathematics Subject Classification: 62M10; 62M20

*Corresponding author: fa.okolie@acu.edu.ng

1 Introduction

Reliable forecasts of rainfall and atmospheric humidity support agricultural planning, flood-risk management, water-resource allocation, and climate adaptation. Tropical climates exhibit pronounced rainfall and humidity cycles, while interactions among rainfall, atmospheric moisture, vegetation, and surface energy create persistent and seasonally varying dependence [1, 2, 3]. Long African climate records also show substantial temporal variation, making stable models important when dependence changes across seasons or regimes [4, 5].

Classical autoregressive models are interpretable and computationally efficient, but fixed seasonal specifications can be inadequate when several frequencies interact. Fourier terms provide a parsimonious representation of recurring behaviour, and previous Fourier autoregressive studies show that harmonic functions can be combined with lagged observations to model seasonal-periodic series [6, 7, 8]. Related environmental-forecasting evidence likewise indicates that forecast performance is series- and horizon-dependent [9].

A difficulty arises when the autoregressive order or the number of harmonics increases. Lagged harmonic regressors then become numerous and can be strongly correlated, so ordinary least-squares estimates may be unstable and highly sensitive to small data perturbations. Ridge regression addresses this problem by shrinking correlated coefficients while retaining the coordinated sine-cosine basis [10, 11]. Recent environmental applications also demonstrate the usefulness of regularisation in high-dimensional forecasting systems [12, 13].

Modern forecasting research continues to exploit frequency-domain information, including Fourier-based neural architectures and semiparametric spline-Fourier climate models [14, 15]. Nevertheless, a flexible forecasting model should be evaluated against simple, credible benchmarks and selected without using the test period. Information criteria alone can favour an over-parameterised model with poor multi-step forecasting behaviour, particularly when the design matrix is ill-conditioned.

This study therefore develops a ridge-penalised Fourier autoregressive model (Ridge-PFAR) for monthly Nigerian rainfall and relative humidity. Its contribution is threefold. First, it provides a unified penalised formulation containing additive Fourier terms and lag-harmonic interactions. Second, it evaluates FAR and Ridge-PFAR in a controlled simulation in which the sample size and forecast horizon are fixed while model dimension increases. Third, it searches $p = 1, \dots, 10$ and $K = 1, \dots, 4$ using identical rolling-origin folds, compares the selected models with a seasonal-naive benchmark, and reports numerical stability, residual diagnostics, scale-dependent and scale-free forecast errors, and residual-bootstrap prediction intervals.

2 Methods

2.1 Data and empirical design

The empirical dataset contains 132 monthly observations of rainfall and relative humidity for Nigeria from January 2014 to December 2024, supplied by the Nigerian Meteorological Agency (NIMET). The supplied series contain no missing values. Because station-level identifiers and spatial metadata are unavailable in the supplied dataset, the two variables are analysed as single monthly Nigerian series; consequently, no station-level or spatial interpretation is attempted. The first 108 observations (January 2014–December 2022) form the training sample, while the final 24 observations (January 2023–December 2024) form a strictly held-out test sample.

2.2 Stationarity assessment

Stationarity is assessed using the Augmented Dickey-Fuller (ADF) and Kwiatkowski-Phillips-Schmidt-Shin (KPSS) tests. Their null hypotheses are complementary: the ADF null hypothesis is a unit root, whereas the KPSS null hypothesis is stationarity. For a series y_t, the ADF regression is

$$\Delta y_t = \vartheta + \psi y_{t-1} + \sum_{i=1}^{k} \omega_i \Delta y_{t-i} + \xi_t, \tag{1}$$

where rejection of $H_0 : \psi = 0$ supports stationarity. The KPSS statistic is

$$\mathrm{KPSS} = \frac{1}{T^2 \widehat{\sigma}^2_{\mathrm{LR}}} \sum_{t=1}^{T} S_t^2, \qquad S_t = \sum_{i=1}^{t} \widehat{\varepsilon}_i, \tag{2}$$

where $\widehat{\sigma}^2_{\mathrm{LR}}$ estimates the long-run variance. Large KPSS values provide evidence against stationarity. Because the two tests can lead to inconclusive combinations of decisions, the results are interpreted jointly rather than used as a mechanical differencing rule. The empirical forecasting models are fitted in levels so that forecasts and physical constraints remain directly interpretable.

2.3 Fourier autoregressive model

Let the seasonal period be $\Omega = 12$, and define

$$c_{kt} = \cos\left(\frac{2\pi kt}{\Omega}\right), \qquad s_{kt} = \sin\left(\frac{2\pi kt}{\Omega}\right), \qquad k = 1, \ldots, K.$$

For autoregressive order p and harmonic order K, the model is

$$y_t = \beta_0 + \sum_{k=1}^{K} (a_k c_{kt} + b_k s_{kt}) + \sum_{j=1}^{p} \phi_j y_{t-j} + \sum_{j=1}^{p} \sum_{k=1}^{K} y_{t-j} (\gamma_{jk} c_{kt} + \delta_{jk} s_{kt}) + \varepsilon_t. \tag{3}$$

The additive Fourier terms represent recurring seasonal means, the ordinary lag terms represent persistence, and the lag-harmonic interactions allow the autoregressive effects to vary periodically. Including the intercept, the number of coefficients is

$$q = 1 + 2K + p + 2pK.$$

Writing (3) in matrix form as $y = X\beta + \varepsilon$, the FAR estimator is defined by

$$\widehat{\beta}_{\mathrm{FAR}} = \arg\min_{\beta} \|y - X\beta\|_2^2, \tag{4}$$

which equals $(X^\top X)^{-1} X^\top y$ when $X^\top X$ is nonsingular; a stable numerical least-squares solution is used otherwise.

For Ridge-PFAR, the non-intercept columns are standardised using training-sample means and standard deviations. If X_s denotes the resulting design matrix with an unstandardised intercept column and standardised slope columns, then

$$\widehat{\beta}_\lambda = (X_s^\top X_s + \lambda P)^{-1} X_s^\top y, \qquad P = \mathrm{diag}(0, 1, \ldots, 1), \tag{5}$$

so that the intercept is not penalised. The same training-sample scaling is used when constructing validation and forecast regressors. Numerical instability is summarised by the condition number of the standardised slope normal equations before regularisation and of the corresponding ridge-adjusted normal equations after regularisation.

2.4 Model selection and forecasting

Every combination $p = 1, \dots, 10$ and $K = 1, \dots, 4$ is evaluated. FAR and Ridge-PFAR use the same four expanding-window validation origins at months 60, 72, 84, and 96, each followed by a 12-month recursive forecast. Ridge penalties are searched on a logarithmically spaced grid from 10^{-6} to 10^{10}. The specification with the lowest mean validation RMSE is refitted to all 108 training observations before the 24-month test forecast is produced. This identical-fold design ensures that FAR and Ridge-PFAR are compared using the same temporal information.

AIC and BIC are also computed, up to the common Gaussian-likelihood constant, as

$$\mathrm{AIC} = n \log(\mathrm{RSS}/n) + 2d, \qquad \mathrm{BIC} = n \log(\mathrm{RSS}/n) + d \log n, \tag{6}$$

where $d = q$ for FAR and $d = \mathrm{tr}(H_\lambda)$ for Ridge-PFAR, with

$$H_\lambda = X_s (X_s^\top X_s + \lambda P)^{-1} X_s^\top.$$

Saturated unpenalised fits with $n \le d + 1$ are excluded from information-criterion comparisons. Because likelihood-based information criteria for penalised models require care, AIC and BIC are treated as descriptive diagnostics; rolling-origin forecast accuracy determines the reported forecasting models.

Training-sample goodness of fit is summarised by

$$R^2 = 1 - \frac{\mathrm{RSS}}{\mathrm{TSS}}, \qquad \overline{R}^2 = 1 - (1 - R^2)\frac{n-1}{n-d}, \tag{7}$$

where d is the ordinary parameter count for FAR and the effective degrees of freedom for Ridge-PFAR. These statistics describe in-sample fit and complement, rather than replace, rolling-origin validation RMSE.

The seasonal-naive benchmark is $\widehat{y}_t = y_{t-12}$. For a forecast horizon of length h, forecast accuracy is assessed by

$$\mathrm{RMSE} = \left\{ \frac{1}{h} \sum_{i=1}^{h} (y_i - \widehat{y}_i)^2 \right\}^{1/2}, \tag{8}$$

$$\mathrm{MAE} = \frac{1}{h} \sum_{i=1}^{h} |y_i - \widehat{y}_i|, \tag{9}$$

$$\mathrm{sMAPE} = \frac{200}{h} \sum_{i=1}^{h} \frac{|y_i - \widehat{y}_i|}{|y_i| + |\widehat{y}_i|}, \tag{10}$$

and

$$\mathrm{MASE} = \frac{h^{-1} \sum_{i=1}^{h} |y_i - \widehat{y}_i|}{(T-12)^{-1} \sum_{t=13}^{T} |y_t - y_{t-12}|}. \tag{11}$$

For sMAPE, a term with $y_i = \widehat{y}_i = 0$ is defined to contribute zero, thereby avoiding the 0/0 indeterminacy that can occur for zero rainfall. MASE directly compares absolute forecast error with the in-sample seasonal-naive scale.

Recursive predictions are constrained to physically meaningful ranges: rainfall forecasts are truncated at zero and relative-humidity forecasts to $[0, 100]$. For Ridge-PFAR, 95% prediction intervals are obtained from 2,000 recursive residual-bootstrap paths using the same physical bounds. Residual autocorrelation is assessed using the Ljung-Box test through lag 12.

2.5 Monte Carlo design

The simulation fixes $T = 144$, with a 120-observation training sample, a 24-step forecast horizon, innovation variance equal to one, and seasonal period 12. Complexity increases through $(p, K) = (2, 1)$, $(6, 2)$, and $(10, 4)$, corresponding to 8, 34, and 98 non-intercept slope regressors, respectively. Data are generated from stable versions of (3), with decreasing lag coefficients and progressively richer lag-harmonic interactions. Each scenario uses 500 independent replications. Ridge penalties are selected using an internal 24-observation validation block within the training sample; the final 24 observations are reserved exclusively for forecast evaluation. The reported summaries include mean and median RMSE, the standard deviation of RMSE, median normal-equation condition numbers before and after penalisation, and the median selected penalty.

3 Results

3.1 Descriptive and stationarity results

The monthly series exhibit substantial heterogeneity (Table 1). Rainfall is highly variable and right-skewed, whereas relative humidity is smoother and bounded. Figure 1 shows clear recurring structure in both targets.

Table 1: Descriptive statistics for the 132 monthly observations.

Variable	Mean	SD	Minimum	Maximum	Skewness	Kurtosis
Rainfall (mm)	99.62	95.21	0.00	370.80	0.66	-0.59
Relative humidity (%)	75.01	11.00	39.00	88.00	-1.12	0.73

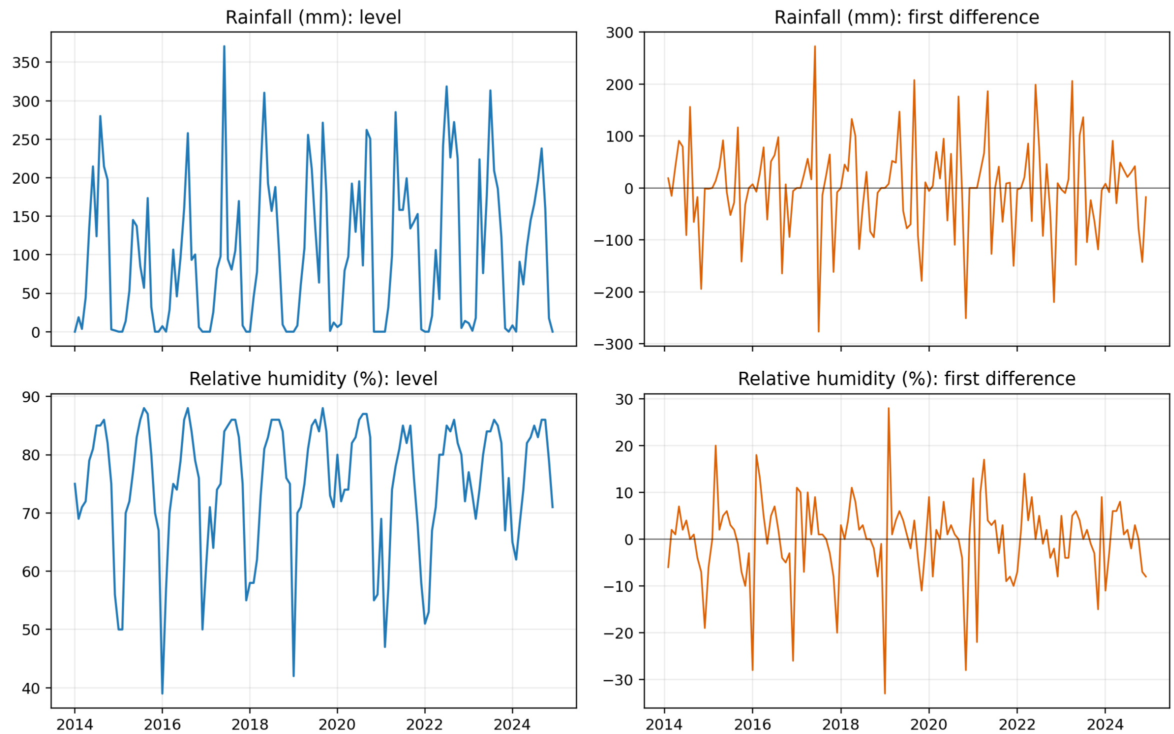

Figure 1: Monthly rainfall and relative humidity in levels and first differences, January 2014–December 2024.

The ADF and KPSS tests give inconclusive combinations of evidence in levels (Table 2): the ADF test does not reject a unit root, while the KPSS test does not reject stationarity. First differences strongly reject the ADF unit-root null and do not reject the KPSS stationarity null. The forecasting models nevertheless remain in levels to preserve seasonal information and direct physical interpretation.

Table 2: Stationarity tests for the target series.

Series	Form	ADF statistic	ADF p	KPSS statistic	KPSS p
Rainfall	Level	-1.8846	0.3393	0.1449	0.1000
Rainfall	First difference	-8.6017	0.0000	0.0368	0.1000
Relative humidity	Level	-2.4444	0.1296	0.0746	0.1000
Relative humidity	First difference	-10.6882	0.0000	0.0125	0.1000

3.2 Simulation results

Table 3 and Figure 2 show that ridge regularisation has little cost in the low- and moderate-dimensional designs and becomes especially valuable in the high-dimensional design. High-dimensional FAR has a median RMSE of 10.9645, but a small number of explosive forecasts raise its mean RMSE to 2621.5584 and its RMSE standard deviation to 40899.3371. Ridge-PFAR reduces the median and mean RMSE to 1.1576 and 1.1874, respectively, while reducing the median normal-equation condition number from 3049.0586 to 7.2537.

Table 3: Monte Carlo results from 500 replications.

Scenario	Method	Regressors	Mean RMSE	Median RMSE	RMSE SD	Unpen. condition	Penalised condition	Median λ
Low	FAR	8	1.1379	1.1163	0.2122	6.6747	6.6747	0
Low	Ridge-PFAR	8	1.1474	1.1337	0.2133	6.6747	5.1194	3.1623
Moderate	FAR	34	1.1165	1.1013	0.2009	29.2166	29.2166	0
Moderate	Ridge-PFAR	34	1.1173	1.1015	0.1945	29.2166	10.7152	31.6228
High	FAR	98	2621.5584	10.9645	40899.3371	3049.0586	3049.0586	0
High	Ridge-PFAR	98	1.1874	1.1576	0.3238	3049.0586	7.2537	100.0000

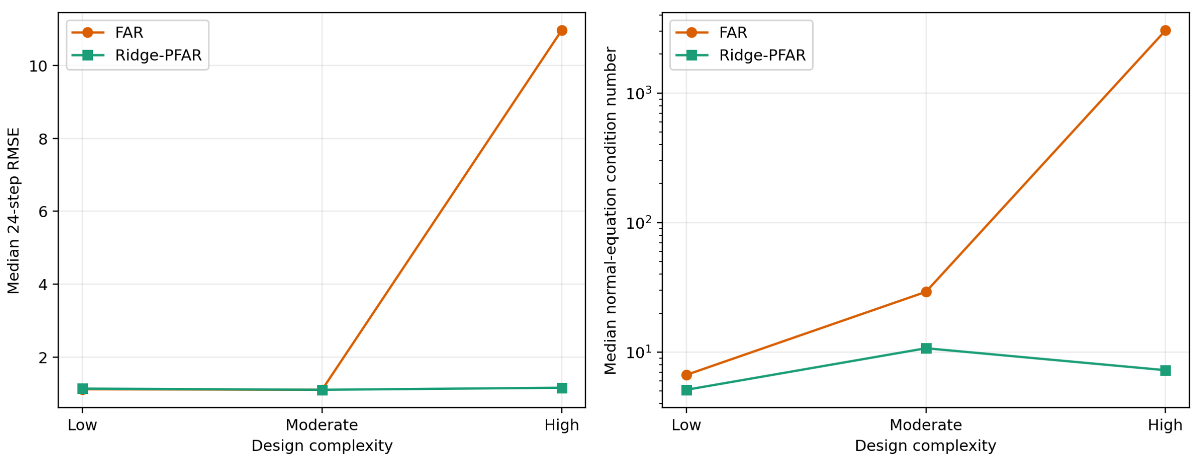

Figure 2: Median Monte Carlo forecast RMSE and normal-equation conditioning across increasing model dimension.

3.3 Empirical model selection and forecasts

Information criteria and rolling validation do not select the same models (Table 4). AIC repeatedly favours very large unpenalised FAR specifications, whereas BIC and rolling validation favour more parsimonious models. This divergence supports the use of temporally ordered validation for the forecasting comparison rather than treating the AIC-minimising model as the preferred forecaster.

Table 4: Best empirical specifications under AIC, BIC, and rolling-origin validation.

Target	Method	Criterion	p	K	λ
Rainfall	FAR	AIC	9	4	0
Rainfall	FAR	BIC	1	1	0
Rainfall	FAR	Validation RMSE	1	3	0
Rainfall	Ridge-PFAR	AIC	1	2	2.5119
Rainfall	Ridge-PFAR	BIC	1	2	2.5119
Rainfall	Ridge-PFAR	Validation RMSE	2	4	1.0000
Relative humidity	FAR	AIC	9	4	0
Relative humidity	FAR	BIC	1	1	0
Relative humidity	FAR	Validation RMSE	1	1	0
Relative humidity	Ridge-PFAR	AIC	1	2	15.8489
Relative humidity	Ridge-PFAR	BIC	1	2	15.8489
Relative humidity	Ridge-PFAR	Validation RMSE	2	2	39.8107

The held-out results are reported in Table 5. The fitted R^2 and adjusted R^2 values show that the selected models explain substantial training-sample variation, particularly for relative humidity. For rainfall, FAR gives the lowest test RMSE (53.8078), although Ridge-PFAR was preferred by rolling validation and both fitted models improve on the seasonal-naive benchmark. For relative humidity, Ridge-PFAR performs best on every reported test metric, reducing RMSE from 6.2069 for FAR and 8.2031 for the seasonal-naive method to 5.8410. Thus, regularisation provides a clear humidity gain, whereas the rainfall ranking changes between validation and the final test period.

Table 5: Rolling-selected models and 24-month test performance.

Target	Method	p	K	λ	R^2	Adj. R^2	CV RMSE	Test RMSE	MAE	sMAPE	MASE
Rainfall	Seasonal naive	–	–	–	–	–	–	60.7139	43.8083	76.8390	0.7489
Rainfall	FAR	1	3	0	0.6238	0.5656	69.5154	53.8078	38.3855	59.3762	0.6562
Rainfall	Ridge-PFAR	2	4	1.0000	0.7016	0.6117	67.6024	56.6733	39.1393	68.4788	0.6691
Relative humidity	Seasonal naive	–	–	–	–	–	–	8.2031	4.7917	7.1793	0.8503
Relative humidity	FAR	1	1	0	0.7377	0.7235	7.2870	6.2069	4.3322	6.1029	0.7688
Relative humidity	Ridge-PFAR	2	2	39.8107	0.7389	0.7266	7.1687	5.8410	3.9612	5.5316	0.7029

Table 6 distinguishes the unpenalised normal-equation condition number from the condition number after applying the selected ridge penalty. For the selected rainfall ridge model, penalisation reduces the condition number from 2520.3107 to 375.6988; for relative humidity, it falls from 15074.6004 to 11.8748. Ljung-Box tests through lag 12 do not reject the null hypothesis of no residual autocorrelation at the 5% level for any selected fitted model. Residual-bootstrap coverage is close to nominal for rainfall but lower for relative humidity, so the latter intervals should be interpreted cautiously.

Table 6: Diagnostics for the rolling-selected FAR and Ridge-PFAR models.

Target	Method	Unpenalised condition	Penalised condition	Ljung-Box p	95% coverage	Mean interval width
Rainfall	FAR	252.0888	252.0888	0.1308	–	–
Rainfall	Ridge-PFAR	2520.3107	375.6988	0.0915	0.9583	255.1672
Relative humidity	FAR	1097.3939	1097.3939	0.6687	–	–
Relative humidity	Ridge-PFAR	15074.6004	11.8748	0.7301	0.8750	27.8927

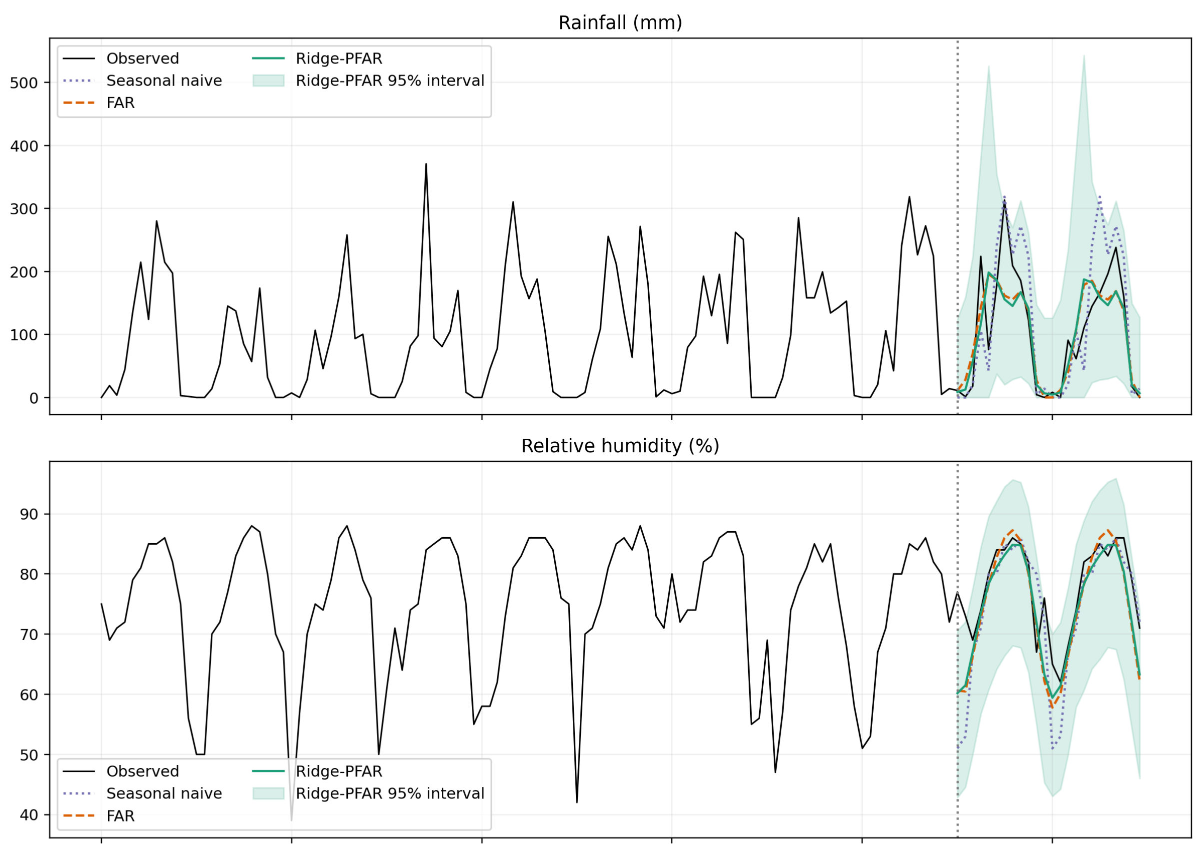

Figure 3: Observed test values, seasonal-naive forecasts, and rolling-selected FAR and Ridge-PFAR forecasts. Shading denotes Ridge-PFAR 95% residual-bootstrap intervals.

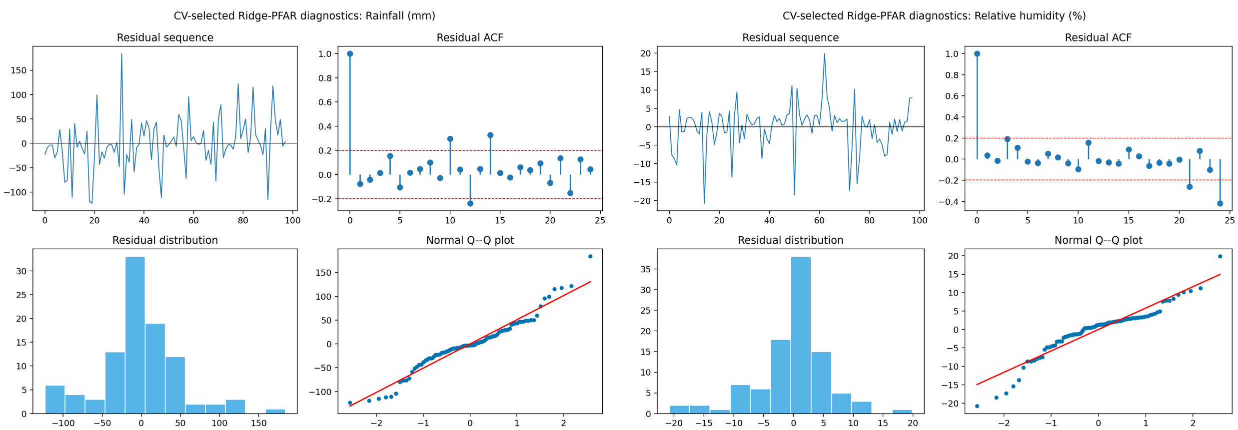

Figure 4: Residual diagnostics for the rolling-selected Ridge-PFAR models: rainfall (left) and relative humidity (right).

4 Discussion

The simulation isolates the role of dimensionality: with sample size, innovation scale, and forecast horizon held fixed, unpenalised FAR deteriorates sharply when the number of correlated regressors becomes large. Ridge-PFAR remains stable across all three designs. This behaviour is consistent with the classical bias-variance rationale for ridge regression [10, 11] and with recent regularised environmental forecasting applications [12, 13].

The empirical results are more nuanced. Ridge-PFAR is preferred by rolling validation for both targets, but FAR obtains the lower rainfall test error, whereas Ridge-PFAR clearly improves relative-humidity forecasts. This target- and period-specific result is more credible than a universal superiority claim and is consistent with broader environmental forecasting comparisons showing that no single method dominates every series [9]. The seasonal-naive comparison remains important: both fitted models add value for both targets, with the largest relative gain occurring for relative humidity under Ridge-PFAR.

The residual diagnostics in Figure 4 complement the Ljung-Box results. Although there is no statistically significant evidence of residual autocorrelation through lag 12 at the 5% level, the normal Q-Q plots show noticeable tail departures, particularly for rainfall. Thus, the residual-bootstrap intervals should be interpreted as practical forecast intervals rather than as evidence of an exact Gaussian error model.

Several limitations remain. The dataset is short, covers only 11 years, and lacks station identifiers and spatial metadata, so spatial heterogeneity cannot be assessed. Forecast intervals are based on residual resampling and have sub-nominal coverage for relative humidity. The empirical search is finite, physical bounds are imposed by truncation rather than by a distribution tailored to nonnegative rainfall or bounded proportions, and no external climate covariates are used. Future work should evaluate spatial or station-level data, transformed or distributional models, alternative penalties, and interval procedures that better represent heteroscedasticity and extremes.

5 Conclusion

Ridge regularisation provides an effective safeguard when Fourier autoregression becomes high-dimensional and ill-conditioned. In simulation, Ridge-PFAR prevents the explosive forecast failures observed for high-dimensional FAR. In the Nigerian application, Ridge-PFAR improves relative-humidity forecasts, while FAR has the lower rainfall test error despite Ridge-PFAR's better rainfall validation score. Both fitted methods outperform the seasonal-naive benchmark for both targets. The evidence therefore supports Ridge-PFAR as a stable extension of Fourier autoregression, but not as a universally superior forecasting method.

Acknowledgements

The authors acknowledge the Nigerian Meteorological Agency (NIMET) as the stated source of the climate observations used in this study.

Conflict of Interest

The authors declare no competing financial interests or personal relationships that could have influenced this work.

Funding

No external funding was received for this research.

Data Availability

The empirical data were supplied by NIMET. Redistribution and access are subject to the data provider's permission.

Code Availability

The analysis scripts used to generate the simulation and empirical results accompany the manuscript files.

References

[1] Met Office. (2024). Understanding humidity. *Met Office*. Available at: `https://weather.metoffice.gov.uk/learn-about/weather/types-of-weather/humidity`

[2] Borma, L. S., Costa, M. H., da Rocha, H. R., Arieira, J., Nascimento, N. C. C., Jaramillo-Giraldo, C., *et al.* (2022). Beyond carbon: The contributions of South American tropical humid and subhumid forests to ecosystem services. *Reviews of Geophysics*, 60(4), e2021RG000766. doi:10.1029/2021RG000766

[3] Jackson, L. S., Birch, C. E., Chagnaud, G., Marsham, J. H., & Taylor, C. M. (2025). Daily rainfall variability controls humid heatwaves in the global tropics and subtropics. *Nature Communications*, 16(1), 3461. doi:10.1038/s41467-025-58694-6

[4] Gil-Alana, L. A., Yaya, O. S., & Fagbamigbe, A. F. (2019). Time series analysis of quarterly rainfall and temperature (1900–2012) in sub-Saharan African countries. *Theoretical and Applied Climatology*, 137(1–2), 61–76. doi:10.1007/s00704-018-2583-5

[5] Zhou, S., Yu, B., Lintner, B. R., Findell, K. L., & Zhang, Y. (2023). Projected increase in global runoff dominated by land surface changes. *Nature Climate Change*, 13(5), 442–449. doi:10.1038/s41558-023-01659-8

[6] Taiwo, A. I., Olatayo, T. O., Adedotun, A. F., & Adesanya, K. K. (2019). Modeling and forecasting periodic time series data with Fourier autoregressive model. *Iraqi Journal of Science*, 60(6), 1367–1373. doi:10.24996/ijs.2019.60.6.20

[7] Taiwo, A. I., Olatayo, T. O., & Agboluaje, S. A. (2020). Time series model building with Fourier autoregressive model. *South African Statistical Journal*, 54(2), 243–254. doi:10.37920/sasj.2020.54.2.8

[8] Taiwo, A. I. (2025). An autoregressive process with Fourier terms for seasonal-periodic time series datasets. *Journal of Probability and Statistical Science*, 23(1), 63–76. doi:10.37119/jpss2025.v23i1.830

[9] Effrosynidis, D., Spiliotis, E., Sylaios, G., & Arampatzis, A. (2023). Time series and regression methods for univariate environmental forecasting: An empirical evaluation. *Science of the Total Environment*, 875, 162580. doi:10.1016/j.scitotenv.2023.162580

[10] Hoerl, A. E., & Kennard, R. W. (1970). Ridge regression: Biased estimation for nonorthogonal problems. *Technometrics*, 12(1), 55–67. doi:10.1080/00401706.1970.10488634

[11] Hastie, T., Tibshirani, R., & Wainwright, M. (2015). *Statistical Learning with Sparsity: The Lasso and Generalizations*. CRC Press. doi:10.1201/b18401

[12] Samadi-Koucheksaraee, A., & Chu, X. (2024). Development of a novel modeling framework based on weighted kernel extreme learning machine and ridge regression for streamflow forecasting. *Scientific Reports*, 14, 30910. doi:10.1038/s41598-024-81779-z

[13] Kordani, M., Bagheritabar, M., Ahmadianfar, I., & Samadi-Koucheksaraee, A. (2025). Forecasting water quality indices using generalized ridge model, regularized weighted kernel ridge model, and optimized multivariate variational mode decomposition. *Scientific Reports*, 15, 16313. doi:10.1038/s41598-025-99341-w

[14] Jin, Y., Mao, Y., & Chen, G. (2025). DFCNformer: A Transformer framework for non-stationary time-series forecasting based on de-stationary Fourier and coefficient network. *Information*, 16(1), 62. doi:10.3390/info16010062

[15] Dani, A. T. R., Chamidah, N., Budiantara, I. N., Lestari, B., & Aydin, D. (2026). New statistical approach to forecasting Earth's skin temperature from MERRA-2 satellite using semiparametric time series regression with mixed additive spline Fourier (STSR-MASF). *Forecasting*, 8(1), 6. doi:10.3390/forecast8010006